Research Article | Vol. 31, No. 17 / 14 Aug 2023 / Optics Express 27324
Optics EXPRESS

Slot driven dielectric electromagnetically induced transparency metasurface

THEODORE A. NDUKAIFE AND SUI YANG*

Materials Science and Engineering, School for Engineering of Matter, Transport and Energy, Arizona State University, Tempe, AZ 85287, USA
*suiyang@asu.edu

Abstract: The control of resonant metasurface for electromagnetically induced transparency (EIT) offers unprecedented opportunities to tailor lightwave coupling at the nanoscale leading to many important applications including slow light devices, optical filters, chemical and biosensors. However, the realization of EIT relies on the high degree of structural asymmetry by positional displacement of optically resonant structures, which usually lead to low quality factor (Q-factor) responses due to the light leakage from structural discontinuity from asymmetric displacements. In this work, we demonstrate a new pathway to create high quality EIT metasurface without any displacement of constituent resonator elements. The mechanism is based on the detuning of the resonator modes which generate dark-bright mode interference by simply introducing a slot in metasurface unit cells (meta-atoms). More importantly, the slot diameter and position on the meta-atom can be modulated to tune the transmittance and quality factor (Q-factor) of the metasurface, leading to a Q-factor of 1190 and near unity transmission at the same time. Our work provides a new degree of freedom in designing optically resonant elements for metamaterials and metasurfaces with tailored wave propagation and properties.

1. Introduction

Metasurfaces consisting of thin layers of resonant optical components introduce a new dimension to modulate the behaviors of light. In contrast to conventional optics, metasurfaces are based on artificial nanostructures that can resonantly capture and sculpture light with unprecedented wave propagations [1–6]. These nanostructures can be tailored by their unit structural elements (meta-atoms), which can shape the lightwave with a defined amplitude, phase, polarization, and spectrum through resonant antenna or scattering effects (eg. plasmonic or Mie scattering). By properly designing the structure and arrangement of meta-atoms, metasurfaces have shown unique capabilities for absorbing, concentrating, dispersing, or guiding waves for a plethora of applications such as flat metalens [7–9], wave plates [10–12], cloaking devices [5,13,14], sensors [15–17], beam steering [6,18,19], optical modulators and holograms [20–25]. All these applications can be realized by only a thin layer of metasurface structure, providing insurmountable advantages for integrated photonic systems that surpass conventional bulky optical elements. As demonstrated, metasurfaces have offered a promising avenue to control the extraordinary wave propagation and spectral selectivity. One of the unique wave propagations to explore is electromagnetically induced transparency (EIT), a quantum mechanical interference phenomenon [26], which manifests a transparency window in an otherwise optically opaque medium, promising many fascinating applications such as light storage, slow-light devices, optical sensing and detecting in harsh environment [27–33].

The principle of photonic EIT is based on the destructive interference effect between optical excitation pathways with distinct transition probability amplitude of different resonant optical states [34–38]. In order to achieve this phenomenon, the structural asymmetry of resonant optical elements is essential. For example, EIT was observed in stacked plasmonic optical metamaterial by displacement of the dipole antenna relative to the symmetry axis of the quadrupole antenna

#488704 https://doi.org/10.1364/OE.488704
Journal © 2023 Received 7 Mar 2023; revised 13 Jun 2023; accepted 7 Jul 2023; published 1 Aug 2023

Optics EXPRESS

[34,35]. Here, the coupling strength increases as the displacement between the two resonators is increased, leading to more pronounced transmission window. With the broken symmetries, EIT was further realized in various shaped structures by changing the position of the coupling optical element [39–43]. This changes the coupling coefficient and results in decreases in the Q factor as the degree of asymmetry increases. However, all these nanophotonic EIT media are heavily relied on degree of structural asymmetry with changing the position of one or more resonators relative to others. Although the coupling between the optical states increases with the increase degree of structural asymmetry, it inevitably leading to a lower quality factor (Q-factor) due to the fact that optical damping rate is inversely proportional to the coupling coefficient [43–48]. Moreover, the nanoscale size of resonator elements makes it challenging to fabricate several complex structures with varying degree of structural asymmetry. All of these preclude the realization and applications of high quality (Q-factor) EIT phenomenon ranging from chemical/biological sensing [37,49], narrowband filters [50,51], enhanced nonlinear interactions [52,53] and low loss slow light devices for information storage and communications [30,45,54].

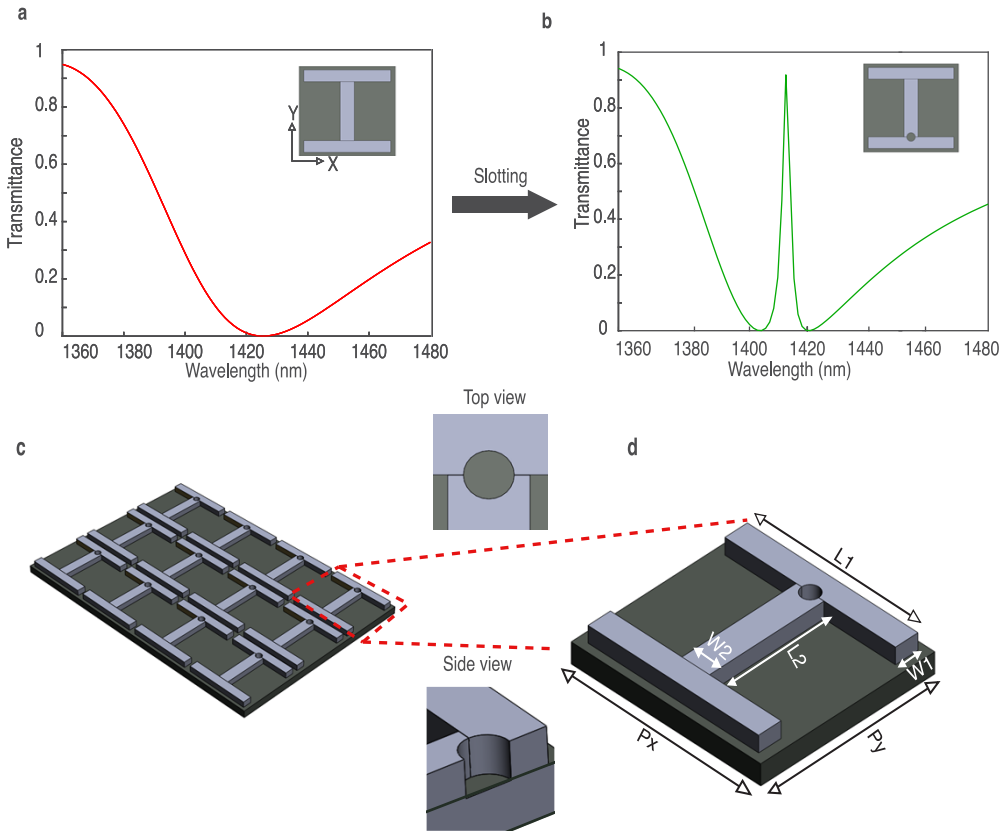

Fig. 1. The design of slot driven EIT metasurface. (a) broad resonance dip in non-slotted metasurface due to excitation of bright modes by the incident field, with k//z, E//y, H//x. (b) EIT properties in slotted metasurface due to interference between bright mode and slot induced dark modes without breaking positional symmetry, (c) schematic a metasurface device where L1 = 960 nm, L2 = 590 nm, w2 = 200[nm], w1 = 160[nm], Px = Py = 1010[nm] utilizing the concept. Top and side views of the slot are shown in the middle inset.

Here we report a new route to achieve EIT by creating the meta-atom states without breaking the positional symmetry of constituent resonators. As a demonstration, we utilize silicon, a

Optics EXPRESS

dielectric with high refractive index in the optical regime, which can provide well engineered resonances and can applied widely in optical communication and information storage [6,55,56]. The meta-atom takes a 'dumbbell' like symmetric design. The coupling optical states and their transition probability are driven by a slot in the center of the structure without changing the position of any resonator elements (Figure 1). This design features the minimalization of structure asymmetry-optical damping effect that allows the access to both bright and dark modes with low loss. With simply tuning on the slot diameter, the metasurface exhibit high quality EIT transmission (Q-factor of 1190 with unity transmission) can be achieved without breaking the structural symmetry of resonant unit cells.

2. Principle and design method

The symmetric meta-atom consists of three rectangular silicon bar resonators sitting on quartz substrate and connected as shown in the inset of Figure 1(a), similar to a symmetric dumbbell-shape. The two parallel resonators are geometrically similar, and their axis of symmetry coincides with that of the connecting bar. By simply introducing a spherical slot in the dumbbell-shaped resonator, the coupling between the 'optical elements' changes. As shown, in the absence of slot, only the dipole modes in the structure are excited as evident in the broad resonance dip in the transmission spectrum observed at wavelength of ~1420 nm (Fig. 1(a)). This is confirmed by the surface current distribution shown in Fig. S1 in the Supplement 1 which shows typical dipole-like pattern. However, by introducing the slot in the structure, the trapped modes are excited and interferes destructively with the bright mode to create a narrow transparency window as observed in around same wavelength, exhibiting well distinct EIT property without any positional displacement of the optical elements. The schematic of the specific metasurface structure and unit cell are shown correspondingly (Fig. 1(c) and (d)). The design parameters of the structure are L1 = 960 nm, L2 = 590 nm, w1 = 160 nm, w2 = 200 nm, the lattice constant in x and y directions (Px = Py = 1010 nm). All the resonators have a subwavelength thickness of 110 nm in which the unit cell structures repeatedly consist of a metasurface in plane.

In a traditional EIT structure, the electromagnetic interference among a three-level system (resonant states in optical elements) is necessary where a metastable energy state is created by relative positional displacement of optical elements [26,28,35,44]. However, the broken symmetry in position inevitably generates large optical damping due to the light leakage from structural discontinuity from asymmetric displacement edges usually leading to a lower Q-factor [43–48]. These design features based on positional displacement limit active tuning capability and practical applications of EIT phenomena. Here we report a simple slot configuration that can induced high quality EIT without any displacement of constituent optical elements or resonators.

The slot EIT principle is based on a trapping mode from the induced slot, which act as the metastable state. In this new three-level system (Fig. 2(a)), the ground state is represented by state $|0\rangle$ and two higher states are $|1\rangle$ and $|2\rangle$. The transition $|0\rangle$ — $|1\rangle$ is a dipole allowed transition and represents the excitation of dipole modes by the incident electric field. In contrast, $|0\rangle$ — $|2\rangle$ is not dipole allowed but can be excited in the structure when the slot is present (subradiant dark trapping mode). Hence, the two possible pathways are $|0\rangle$ — $|1\rangle$ and $|0\rangle$ — $|1\rangle$ — $|2\rangle$ — $|1\rangle$ interfere destructively to create a narrow transparency window. The size of the slot determines the mode level, and the slot position affects the coupling coefficient. Therefore, by tuning these two parameters, the simultaneous high-quality factor and transmission amplitude can be achieved. The tuning of the transparency window characteristics is represented by the upper and lower sates $|2\rangle$ and dotted lines as depicted in Fig. 2(a) (Also see Supplement 1, section 1). Correspondingly, these mode interferences are confirmed by the surface current distribution along the designed slot EIT structure. Figure 2(b) shows the surface current distribution for dipole allowed transition $|0\rangle$ — $|1\rangle$. As expected, only the middle resonator is excited while the two parallel resonators are not as strongly excited since they are not coupled to free space. Yet at the transmission peak,

Optics EXPRESS

the parallel resonators are excited and the opposing currents on top and bottom of the structure destructively interfere as shown in Fig. 2(c) to create an EIT -like spectra. This is evident by the suppression of induced current in the middle bar and simultaneous localization of current in the parallel resonators, well conformed to the electric and magnetic field distribution as well (Supplement 1, Fig. S4).

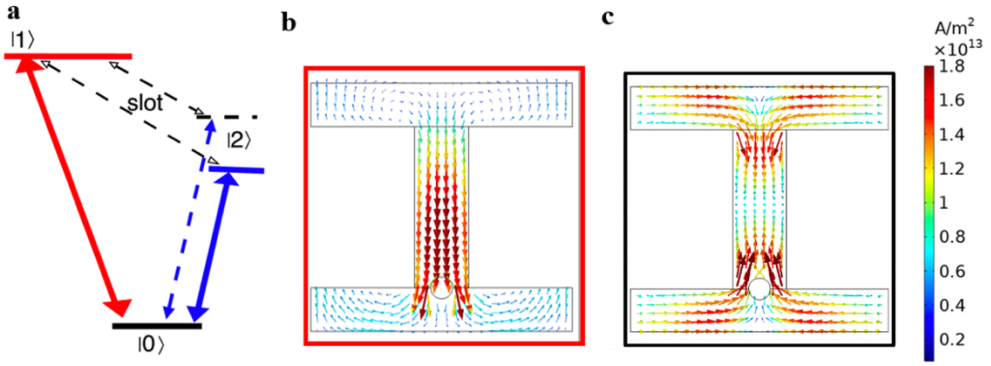

Fig. 2. The principle of Slot driven EIT metasurface (a) interference paths to create EIT through slot mode design. The slot induced EIT mode interference is confirmed by (b) Surface current distribution for path $|0\rangle$ —$|1\rangle$ **(c)** Surface current distribution at the EIT peak follows the path $|0\rangle$ —$|1\rangle$ —$|2\rangle$—$|1\rangle$ due to the interference between slot induced modes.

3. Results and discussion

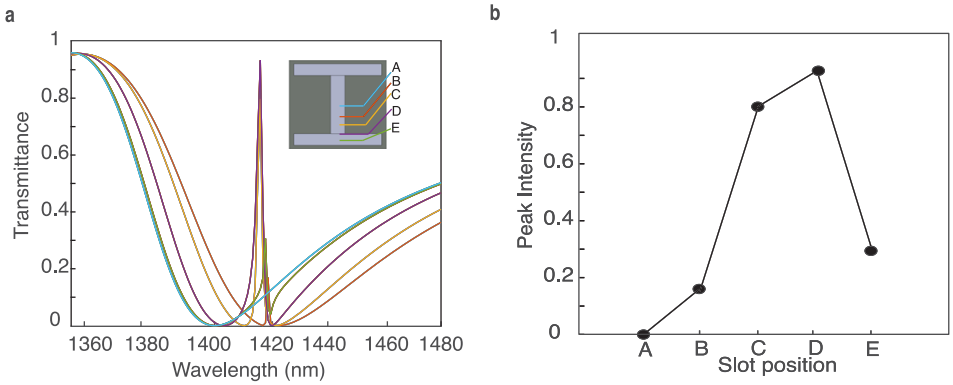

Fig. 3. Transmission characteristic designed by slot located on metasurface structure. The coupling between dark trapping modes (induced by the slot) dipolar resonance mode of the silicon bar resonators is affected by the mode overlapping and hence a function of slot locations. (a) The transmission intensity is zero with the slot centrally located on the structure (A point), increases as we move the slot away from the center and gradually diminishes (b) at point D, the maximum transmission intensity is achieved due to the maximum mode coupling.

To further understand the slot driven transmission characteristics of the metasurface, we have calculated the transmission spectrum as a function of various designed slot locations inside the structure (Fig. 3(a)). The material parameters are taken from amorphous silicon [57] in accordance to the current experimental fabrication situation. As shown, by varying the slot

Optics EXPRESS

location from point A, midpoint of the whole structure to point E (the inset of Fig. 3(a)) while keeping other parameters constant, we observe negligible change in the resonance wavelength and linewidth (Supplement 1, Fig. S8) but a change in transmission intensity. To elucidate the change in transmission, we extract the transmission intensity at resonance wavelength for all slot positions in Fig. 3(b). At position A, which is the midpoint of the structure, the EIT peak is completely suppressed leaving behind a dipole-like resonance dip, hence a transmission intensity of zero. We attribute this to the lack of excitation of the subradiant dark (slot trapping) modes in the structure hence only dipolar resonance is excited by the incident field. To gain further insight into the coupling mechanism, we plotted the current density distribution with the slot at position A and presented the result in Fig. S2(a) in the Supplement 1. The current distribution at the resonance dip confirms our theory that only a dipolar resonance is excited with the slot at this position. The two parallel bars are not excited, rather only the middle connecting bar is excited. As we move away from the center of the structure, and EIT peak appears and the intensity increases. A maximum intensity of 93.5% is achieved at position D. The current distribution at position E presented in Figure S2(b) also confirms the excitation of the parallel resonators as the slot position is changed. This is evidenced by antiparallel current which results in destructive interference of fields created and suppression of radiation. The further discussion on slot position dependent EIT is presented in Supplement 1, section 4.

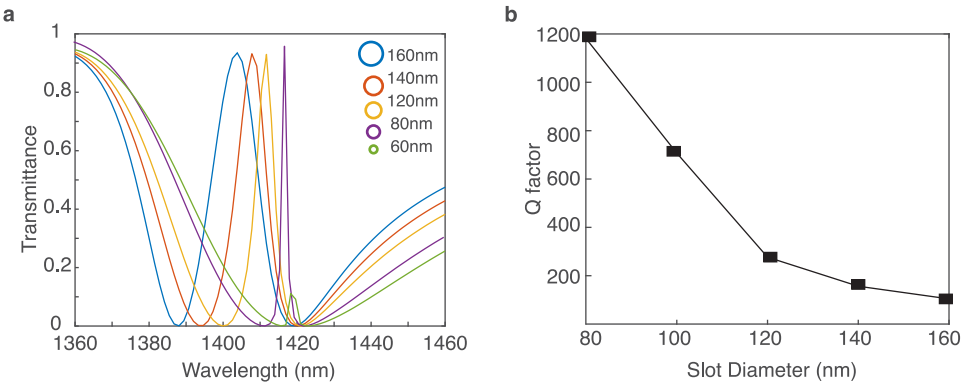

Fig. 4. The control of transmission characteristics by slot size. (a) the transmission spectra as a function of slot size. Both transmission and linewidth can be simply controlled by slot size under the mode coupling design. At the slot size of 80 nm, the near unity transmission and high Q-factor (b) can be achieved at the same time.

Besides, the size of the slot determines the mode level and thus can affect the strength of destructive interferences as well as the linewidth of the transmission spectrum. To understand the size effect, we varied the slot diameter in steps of 20 nm from 60 nm to 160 nm at position D with all other parameters constant and plotted the transmission spectrum in Fig. 4(a). Without changing the trend, we have omitted the case where diameter is 100 nm to make it easier to visualize the plot. It is evident that the slot diameter significantly changes the resonance linewidth, and the spectrum is slightly redshifted as the slot diameter decreases. We attribute this decrease in linewidth to the optimized coupling among the resonators which results in suppression of radiative losses. To quantify this dependence of the resonance linewidth on the slot diameter, we extracted the linewidth (Supplement 1, Fig. S9) for each curve in Figure 3(a) and obtained the Q-factor of the metasurface by dividing the full width at half maximum (FWHM) by the resonance wavelength, the results are presented in Fig. 4(b). We have omitted the point where the diameter is 60 nm since the EIT peak is almost suppressed. A maximum Q-factor of 1190 is achieved when the slot diameter is 80 nm and the Q-factor gradually decreases as the slot

Optics EXPRESS

diameter is increased. To elucidate the relationship between the slot diameter and the resonance linewidth, we extracted and plotted the current distributions at the EIT peak. Figure S3(a), in Supplement 1, shows the current distributions at the EIT peak with slot diameter of 160 nm and Fig. 4(b) shows the case where the slot diameter is 80 nm. The distinguished current density distributions between both cases are clearly observed. With a smaller slot diameter of 80 nm the current intensity is greater compared to the when the slot diameter is increased to 160 nm. This shows the transmission peak wavelength and linewidth can be controlled by simply varying the slot diameter. In addition, the results show that the transmission amplitude is not affected by the slot diameter but primarily dependent on the slot position which changes the coupling strength.

4. Conclusion

In summary, we have demonstrated a new pathway to tailor the optical response of a dielectric metasurface to realize EIT in contrast to previous route using positional displacement of the resonators. By controlling the meta-atom states through the introduction of a spherical slot in the structure, the coupling between the bright mode and the subradiant dark (slot trapping) modes can be easily tuned. Moreover, the linewidth and hence Q-factor of our metasurface can be easily modulated by the size of the slot. The demonstrated slot EIT mechanism addresses the light leakage problem by structural displacement edge from traditional EIT design. The work opens new route to design dielectric metasurface with desired resonant effects and wave propagations for important applications such as ultrasensitive chemical/biological sensors, high quality filters, information storage and communications. For example, the high sensitivity of chemical/biological sensors can be enhanced by the high Q-factor narrow spectral window based on the tiny frequency shift. Narrowband filters can be achieved with high Q transmissive window. And the extreme dispersion of group velocity can be induced by EIT window, which leads to slow light for specific guided wave for information technologies.

Funding. National Science Foundation (2227650); Gordon and Betty Moore Foundation; 3M Non-Tenured Faculty Award.

Disclosures. The authors declare no conflicts of interest.

Data availability. Data underlying the results presented in this paper are included in this article and supporting information. Further datasets may be obtained from the authors upon reasonable request.

Supplemental document. See Supplement 1 for supporting content.

References

1. Y. Liu and X. Zhang, "Metamaterials: A new frontier of science and technology," Chem. Soc. Rev. **40**(5), 2494–2507 (2011).
2. N. Yu, P. Genevet, M. A. Kats, F. Aieta, J.-P. Tetienne, F. Capasso, and Z. Gaburro, "Light propagation with phase discontinuities: generalized laws of reflection and refraction," Science **334**(6054), 333–337 (2011).
3. A. V. Kildishev, A. Boltasseva, and V. M. Shalaev, "Planar photonics with metasurfaces," Science **339**(6125), 12320091 (2013).
4. N. Yu and F. Capasso, "Flat optics with designer metasurfaces," Nat. Mater. **13**(2), 139–150 (2014).
5. X. Ni, Z. J. Wong, M. Mrejen, Y. Wang, and X. Zhang, "An ultrathin invisibility skin cloak for visible light," Science **349**(6254), 1310–1314 (2015).
6. M. I. Shalaev, J. Sun, A. Tsukernik, A. Pandey, K. Nikolskiy, and N. M. Litchinitser, "High-efficiency all-dielectric metasurfaces for ultracompact beam manipulation in transmission mode," Nano Lett. **15**(9), 6261–6266 (2015).
7. S. Wang, P. C. Wu, V. C. Su, Y. C. Lai, M. K. Chen, H. Y. Kuo, B. H. Chen, Y. H. Chen, T. T. Huang, J. H. Wang, R. M. Lin, C. H. Kuan, T. Li, Z. Wang, S. Zhu, and D. P. Tsai, "A broadband achromatic metalens in the visible," Nat. Nanotechnol. **13**(3), 227–232 (2018).
8. P. Lalanne and P. Chavel, "Metalenses at visible wavelengths: past, present, perspectives," Laser Photon. Rev. **11**(3), 1600295 (2017).
9. M. Khorasaninejad, W. T. Chen, R. C. Devlin, J. Oh, A. Y. Zhu, and F. Capasso, "Metalenses at visible wavelengths: Diffraction-limited focusing and subwavelength resolution imaging," Science **352**(6290), 1190–1194 (2016).
10. F. Ding, Z. Wang, S. He, V. M. Shalaev, and A. V. Kildishev, "Broadband high-efficiency half-wave plate: A supercell-based plasmonic metasurface approach," ACS Nano **9**(4), 4111–4119 (2015).

Optics EXPRESS

11. N. Yu, F. Aieta, P. Genevet, M. A. Kats, Z. Gaburro, and F. Capasso, "A broadband, background-free quarter-wave plate based on plasmonic metasurfaces," Nano Lett. **12**(12), 6328–6333 (2012).
12. Y. Zhao and A. Alù, "Manipulating light polarization with ultrathin plasmonic metasurfaces," Phys. Rev. B **84**(20), 205428 (2011).
13. P. Y. Chen, C. Argyropoulos, and A. Alù, "Broadening the cloaking bandwidth with non-foster metasurfaces," Phys. Rev. Lett. **111**(23), 233001 (2013).
14. P. Y. Chen and A. Alù, "Mantle cloaking using thin patterned metasurfaces," Phys. Rev. B **84**(20), 205110 (2011).
15. J. Qin, S. Jiang, Z. Wang, X. Cheng, B. Li, Y. Shi, D. P. Tsai, A. Q. Liu, W. Huang, and W. Zhu, "Metasurface Micro/Nano-Optical Sensors: Principles and Applications," ACS Nano **16**(8), 11598–11618 (2022).
16. A. J. Ollanik, I. O. Oguntoye, G. Z. Hartfield, and M. D. Escarra, "Highly Sensitive, Affordable, and Adaptable Refractive Index Sensing with Silicon-Based Dielectric Metasurfaces," Adv. Mater. Technol. **4**(2), 1800567 (2019).
17. M. S. Faraji-Dana, E. Arbabi, A. Arbabi, S. M. Kamali, H. Kwon, and A. Faraon, "Compact folded metasurface spectrometer," Nat. Commun. **9**(2), 4196 (2018).
18. P. C. Wu, R. A. Pala, G. Kafaie Shirmanesh, W. H. Cheng, R. Sokhoyan, M. Grajower, M. Z. Alam, D. Lee, and H. A. Atwater, "Dynamic beam steering with all-dielectric electro-optic III–V multiple-quantum-well metasurfaces," Nat. Commun. **10**(1), 3654 (2019).
19. Z. Wei, Y. Cao, X. Su, Z. Gong, Y. Long, and H. Li, "Highly efficient beam steering with a transparent metasurface," Opt. Express **21**(9), 10739–10745 (2013).
20. N. Dabidian, I. Kholmanov, A. B. Khanikaev, K. Tatar, S. Trendafilov, S. H. Mousavi, C. Magnuson, R. S. Ruoff, and G. Shvets, "Electrical switching of infrared light using graphene integration with plasmonic Fano resonant metasurfaces," ACS Photonics **2**(2), 216–227 (2015).
21. A. Arbabi, Y. Horie, M. Bagheri, and A. Faraon, "Dielectric metasurfaces for complete control of phase and polarization with subwavelength spatial resolution and high transmission," Nat. Nanotechnol. **10**(11), 937–943 (2015).
22. L. Huang, X. Chen, H. Mühlenbernd, H. Zhang, S. Chen, B. Bai, Q. Tan, G. Jin, K. W. Cheah, C. W. Qiu, J. Li, T. Zentgraf, and S. Zhang, "Three-dimensional optical holography using a plasmonic metasurface," Nat. Commun. **4**(1), 2808 (2013).
23. S. Q. Li, X. Xu, R. M. Veetil, V. Valuckas, R. Paniagua-Domínguez, and A. I. Kuznetsov, "Phase-only transmissive spatial light modulator based on tunable dielectric metasurface," Science **364**(6445), 1087–1090 (2019).
24. G. Zheng, H. Mühlenbernd, M. Kenney, G. Li, T. Zentgraf, and S. Zhang, "Metasurface holograms reaching 80% efficiency," Nat. Nanotechnol. **10**(4), 308–312 (2015).
25. X. Ni, A. V. Kildishev, and V. M. Shalaev, "Metasurface holograms for visible light," Nat. Commun. **4**(1), 2807 (2013).
26. M. Fleischhauer, A. Imamoglu, and P. J. Marangos, "Electromagnetically induced transparency," Rev. Mod. Phys. **77**(2), 633–673 (2005).
27. C. Liu, Z. Dutton, C. H. Behroozi, and L. V. Hau, "Observation of coherent optical information storage in an atomic medium using halted light pulses," Nature **409**(6819), 490–493 (2001).
28. N. Papasimakis, V. A. Fedotov, N. I. Zheludev, and S. L. Prosvirnin, "Metamaterial analog of electromagnetically induced transparency," Phys Rev Lett **101**, 253903 (2008).
29. N. Liu, M. Hentschel, T. Weiss, A. P. Alivisatos, and H. Giessen, "Three-dimensional plasmon rulers," Science **332**(6036), 1407–1410 (2011).
30. A. H. Safavi-Naeini, T. P. M. Alegre, J. Chan, M. Eichenfield, M. Winger, Q. Lin, J. T. Hill, D. E. Chang, and O. Painter, "Electromagnetically induced transparency and slow light with optomechanics," Nature **472**(7341), 69–73 (2011).
31. G. Heinze, C. Hubrich, and T. Halfmann, "Stopped light and image storage by electromagnetically induced transparency up to the regime of one minute," Phys. Rev. Lett. **111**(3), 033601 (2013).
32. T. Nakanishi, T. Otani, Y. Tamayama, and M. Kitano, "Storage of electromagnetic waves in a metamaterial that mimics electromagnetically induced transparency," Phys. Rev. B **87**(16), 161110 (2013).
33. J. Gu, R. Singh, X. Liu, X. Zhang, Y. Ma, S. Zhang, S. A. Maier, Z. Tian, A. K. Azad, H. T. Chen, A. J. Taylor, J. Han, and W. Zhang, "Active control of electromagnetically induced transparency analogue in terahertz metamaterials," Nat. Commun. **3**(1), 1151 (2012).
34. S. Zhang, D. A. Genov, Y. Wang, M. Liu, and X. Zhang, "Plasmon-induced transparency in metamaterials," Phys. Rev. Lett. **101**(4), 047401 (2008).
35. N. Liu, L. Langguth, T. Weiss, J. Kästel, M. Fleischhauer, T. Pfau, and H. Giessen, "Plasmonic analogue of electromagnetically induced transparency at the Drude damping limit," Nat. Mater. **8**(9), 758–762 (2009).
36. M. D. Lukin and A. Imamoğlu, "Controlling photons using electromagnetically induced transparency," Nature **413**(6853), 273–276 (2001).
37. Y. Yang, I. I. Kravchenko, D. P. Briggs, and J. Valentine, "All-dielectric metasurface analogue of electromagnetically induced transparency," Nat. Commun. **5**(1), 5753 (2014).
38. B. Peng, ŞK Özdemir, W. Chen, F. Nori, and L. Yang, "What is and what is not electromagnetically induced transparency in whispering-gallery microcavities," Nat. Commun. **5**(1), 5082 (2014).
39. V. A. Fedotov, M. Rose, S. L. Prosvirnin, N. Papasimakis, and N. I. Zheludev, "Sharp trapped-mode resonances in planar metamaterials with a broken structural symmetry," Phys. Rev. Lett. **99**(14), 147401 (2007).

Optics EXPRESS

40. F. Hao, Y. Sonnefraud, P. Van Dorpe, S. A. Maier, N. J. Halas, and P. Nordlander, "Symmetry breaking in plasmonic nanocavities: Subradiant LSPR sensing and a tunable Fano resonance," Nano Lett. **8**(11), 3983–3988 (2008).
41. K. Aydin, I. M. Pryce, and H. A. Atwater, "Symmetry breaking and strong coupling in planar optical metamaterials," Opt. Express **18**(13), 13407–13417 (2010).
42. B. Han, X. Li, C. Sui, J. Diao, X. Jing, and Z. Hong, "Analog of electromagnetically induced transparency in an E-shaped all-dielectric metasurface based on toroidal dipolar response," Opt. Mater. Express **8**(8), 2197–2207 (2018).
43. P. Tassin, L. Zhang, R. Zhao, A. Jain, T. Koschny, and C. M. Soukoulis, "Electromagnetically induced transparency and absorption in metamaterials: The radiating two-oscillator model and its experimental confirmation," Phys. Rev. Lett. **109**(18), 187401 (2012).
44. R. Singh, C. Rockstuhl, F. Lederer, and W. Zhang, "Coupling between a dark and a bright eigenmode in a terahertz metamaterial," Phys. Rev. B **79**(8), 085111 (2009).
45. P. Tassin, L. Zhang, T. Koschny, E. N. Economou, and C. M. Soukoulis, "Low-loss metamaterials based on classical electromagnetically induced transparency," Phys. Rev. Lett. **102**(5), 053901 (2009).
46. V. A. Fedotov, N. Papasimakis, E. Plum, A. Bitzer, M. Walther, P. Kuo, D. P. Tsai, and N. I. Zheludev, "Spectral collapse in ensembles of metamolecules," Phys. Rev. Lett. **104**(22), 223901 (2010).
47. S. D. Jenkins and J. Ruostekoski, "Metamaterial transparency induced by cooperative electromagnetic interactions," Phys. Rev. Lett. **111**(14), 147401 (2013).
48. R. Taubert, M. Hentschel, and H. Giessen, "Plasmonic analog of electromagnetically induced absorption: Simulations, experiments, and coupled oscillator analysis," J. Opt. Soc. Am. B **30**(12), 3123–3134 (2013).
49. N. Liu, T. Weiss, M. Mesch, L. Langguth, U. Eigenthaler, M. Hirscher, C. Sönnichsen, and H. Giessen, "Planar metamaterial analogue of electromagnetically induced transparency for plasmonic sensing," Nano Lett. **10**(4), 1103–1107 (2010).
50. H. Lu, X. Liu, G. Wang, and D. Mao, "Tunable high-channel-count bandpass plasmonic filters based on an analogue of electromagnetically induced transparency," Nanotechnology **23**(44), 444003 (2012).
51. M. Davanço, P. Holmström, D. J. Blumenthal, and L. Thylén, "Directional coupler wavelength filters based on waveguides exhibiting electromagnetically induced transparency," IEEE J. Quantum Electron. **39**(4), 608–613 (2003).
52. T. Nakanishi and M. Kitano, "Storage and retrieval of electromagnetic waves using electromagnetically induced transparency in a nonlinear metamaterial," Appl. Phys. Lett. **112**(20), 201905 (2018).
53. Y. Sun, Y. W. Tong, C. H. Xue, Y. Q. Ding, Y. H. Li, H. Jiang, and H. Chen, "Electromagnetic diode based on nonlinear electromagnetically induced transparency in metamaterials," Applied Physics Letters 103 (2013).
54. J. Wang, B. Yuan, C. Fan, J. He, P. Ding, Q. Xue, and E. Liang, "A novel planar metamaterial design for electromagnetically induced transparency and slow light," Opt. Express **21**(21), 25159–25166 (2013).
55. A. I. Kuznetsov, A. E. Miroshnichenko, M. L. Brongersma, Y. S. Kivshar, and B. Luk'yanchuk, "Optically resonant dielectric nanostructures," Science 354 (2016).
56. K. Koshelev and Y. Kivshar, "Dielectric Resonant Metaphotonics," ACS Photonics **8**(1), 102–112 (2021).
57. D. T. Pierce and W. E. Spicer, "Electronic structure of amorphous Si from photoemission and optical studies," Phys. Rev. B **5**(8), 3017–3029 (1972).